Dissipative Longitudinal Solitons in a Two-Dimensional Strongly Coupled Complex (Dusty) Plasma

D. Samsonov,* A. V. Ivlev, R. A. Quinn, and G. Morfill
Max-Planck-Institut für Extraterrestrische Physik, D-85740 Garching, Germany

S. Zhdanov
Moscow Engineering Physics Institute, Kashirskoe shosse 31, 115409, Moscow, Russia
(Received 22 December 2001; published 14 February 2002)

Solitary waves are experimentally studied in a monolayer hexagonal dust lattice which is formed from monodisperse plastic microspheres and levitated in the sheath of an rf discharge. It is found that the product of the soliton amplitude and the square of the soliton width is constant as the soliton propagates. The analytical theory describing the experiment is based on the equations of motion written for a linear chain. It takes into account damping, dispersion, and nonlinearity. The numerical simulation of a linear chain produces double solitons like those observed in the experiment.

DOI: 10.1103/PhysRevLett.88.095004 PACS numbers: 52.27.Lw, 05.45.Yv, 52.35.Fp, 52.35.Sb

A wave isolated in space is called a soliton if it retains its shape as it propagates through the medium. It was first observed by Robinson and Russel [1] and described theoretically by Korteweg and de Vries [2]. The existence of solitons in weakly coupled complex (dusty) plasmas was predicted theoretically [3] and considered in a number of publications (see [4] and references therein).

The existence of solitons in a one-dimensional dust lattice was shown in Ref. [5]. Acoustic solitons are also well known in crystalline solids [6] which can be modeled at a kinetic level by dust lattices [7,8].

The experiments were performed in a capacitively coupled rf discharge (Fig. 1) similar to that of Ref. [9]. The discharge chamber had a lower disk electrode and an upper ring electrode. The upper electrode and the chamber were grounded. A rf power of 10 W (measured as forward minus reverse) was applied to the lower electrode. An argon gas flow at a rate of 0.5 sccm maintained the working gas pressure of 1.8 Pa in the chamber. Monodisperse plastic microspheres 8.9 ± 0.1 μm in diameter were levitated in the sheath above the lower electrode forming a monolayer hexagonal lattice. They were confined radially in a bowl-shaped potential formed by a rim on the outer edge of the electrode. The monolayer particle cloud was about 6 cm in diameter and levitated at a height of $\simeq$9 mm above the lower electrode. The particle separation in the lattice was 650 μm at the excitation edge (Fig. 1), 550 μm in the middle and 720 μm at the outer edge. The particles were illuminated by a horizontal thin (0.2–0.3 mm) sheet of light from a doubled Nd:YAG diode pumped laser (532 nm) and imaged by a top view digital video camera at 102.56 frames/s.

A horizontal tungsten wire 0.1 mm in diameter was placed 4 mm below the particle layer and roughly halfway between the center and the edge of the electrode. A similar wire configuration was used previously, in a different apparatus, in the experiments of Ref. [9]. The wire was normally grounded so that it had little influence on the particles. A short negative pulse (-30 V, 100 ms) applied to the wire pushed the particles away, breaking the lattice above the wire and creating a pulsed one-dimensional compressional disturbance propagating horizontally perpendicular to the wire. The lattice also oscillated in the vertical direction with a small amplitude (well within the thickness of the laser sheet) which caused a periodic change of brightness of the particles, but not a loss from the field of view. The parameters of the excitation pulse were selected such that the disturbance propagated to the end of the lattice without being fully damped. It did not melt the lattice. A time interval of about 1 min allowed the lattice to come to an equilibrium between the experimental runs.

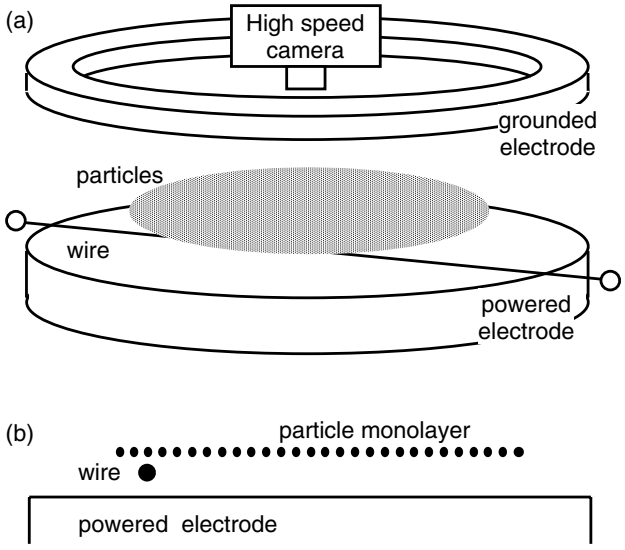

FIG. 1. Sketch of apparatus. (a) Oblique view. Spherical particles charge negatively and form a monolayer levitating in the plasma sheath above the lower electrode. (b) Side view. The grounded wire is placed below the particles. Short negative pulses applied to the wire excite solitons.

In order to analyze the experiments, we identified the particle positions in two consecutive frames to calculate the particle velocities. The areas of Voronoi cells were computed to measure the local particle number density $n(x,t)$ (where x is the distance to the wire and t is time). The measured $n(x,t)$ was averaged in 50 narrow bins parallel to the wire to reduce the influence of random fluctuations.

We visualized the perturbations by plotting a grey-scale map (Fig. 2) of the compression factor $n(x,t)/n_0(x)$ [where $n_0(x)$ is the unperturbed number density]. The lower dark feature corresponds to the studied soliton. Its trajectory is fitted to a theoretical curve (see later) and marked with a dashed curve. The upper dark feature (marked with a dotted line) corresponds to the second weak pulse when the broken dust cloud recollapses. It was used to estimate the dust-lattice wave speed, $C_D L$. In the central region of the lattice this was found to be 23 mm/s (from the slope of the dotted line). The soliton theory predicts that a very weak soliton has Mach number $M = C/C_{DL} \approx 1$, and therefore its propagation speed C is almost equal to the dust-lattice wave speed C_{DL} (note that M always exceeds unity).

We estimated the soliton speed C from the fit to its trajectory (dashed curve in Fig. 2). It decreased as the soliton propagated across the system. C_{DL} is also position dependent since it is a function of the unperturbed number density. It was highest in the middle and slightly lower at the edges. We used the well known theoretical dispersion relation for a 2D dust-lattice wave [10] to get the dependence of C_{DL} on $n_0(x)$ and therefore on x. The resulting Mach number was highest at the excitation edge ($M = 2.1$), decreased to 1.3 in the middle, and rose slightly (to 1.5) at the outer edge.

The soliton theory is based on the equations of motion for a linear chain:

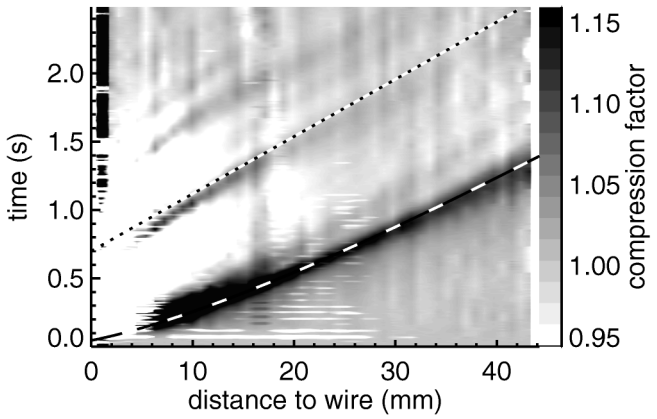

FIG. 2. Compression factor n/n_0 as a function of time and distance to the wire. Darker regions correspond to higher compression. The lower dashed curve is a fit to the trajectory of the soliton. The upper dotted line was drawn above a weak secondary pulse with Mach number $M \approx 1$. Its slope is determined by the dust lattice wave speed $C_{DL} = 23$ mm/s in the middle of the lattice.

$$m\ddot{\mathbf{r}}_k + m\nu_d\dot{\mathbf{r}}_k = -\frac{\partial U_Y}{\partial \mathbf{r}_k} + \mathbf{F}_{\text{ext}},$$
$$U_Y = \sum_{i<j} \frac{Q^2}{r_{ij}} \exp\left(-\frac{r_{ij}}{\lambda_D}\right), \qquad r_{ij} = |\mathbf{r}_i - \mathbf{r}_j|, \quad (1)$$

where $\mathbf{r}_k$ is the particle coordinate, m is the particle mass, $\nu_d = 2.4\ \text{s}^{-1}$ is the damping rate due to the neutral gas friction (Epstein drag), and U_Y is the particle interaction energy in the Yukawa approximation. We assumed that the particle charge Q and the screening length λ_D are constant. The external force $\mathbf{F}_{\text{ext}}$ consists of two components, the stationary confinement force and the nonstationary excitation force. The excitation force acts only during the short time when the pulse is applied to the wire.

We expanded Eqs. (1) using perturbation theory, assuming that the displacement $u(\mathbf{r},t)$ from the equilibrium position is small and keeping the first nonlinear terms. We also made a transition to the continuum limit by assuming that the particle separation is small (long wavelength approximation). The resulting inhomogeneous wave equation, taking into account damping (the second term on the left hand side) as well as nonlinearity and dispersion (the second and the third term on the right hand side), is

$$\frac{\partial^2 u}{\partial t^2} + \nu_d \frac{\partial u}{\partial t} = \kappa \frac{\partial}{\partial x}\left\{\frac{C_{DL}^2}{\kappa}\left[\frac{\partial u}{\partial x} + \frac{\Lambda}{2}\left(\frac{\partial u}{\partial x}\right)^2\right] + \frac{\partial}{\partial x}\left[\frac{C_{DL}^2}{\kappa} l_{\text{disp}}^2 \frac{\partial^2 u}{\partial x^2}\right]\right\} + \frac{F_{\text{ext}}}{m}, \quad (2)$$

where l_{disp} is the dispersion length, and Λ is the dimensionless nonlinearity coefficient. These kinetic coefficients are functions of the lattice parameter $\kappa = a/\lambda_D$, where a is the particle separation. For the inhomogeneous lattice κ depends on x.

For an arbitrary κ, the kinetic coefficients are

$$C_{DL}^2 = \frac{Q^2}{m\lambda_D}\kappa^2[G(\kappa)/\kappa]'',$$
$$l_{\text{disp}}^2 = \frac{1}{12}\lambda_D^2\kappa^2[G''(\kappa)/\kappa]''/[G(\kappa)/\kappa]'',$$
$$\Lambda = \kappa[G(\kappa)/\kappa]'''/[G(\kappa)/\kappa]'',$$

where $G(\kappa) = -\ln(e^\kappa - 1)$, the primes denote derivatives with respect to κ. For $\kappa \gg 1$ we have (nearest neighbor approximation)

$$C_{DL}^2 = \frac{Q^2}{m\lambda_D} e^{-\kappa}(\kappa^2 + 2\kappa + 2)/\kappa,$$
$$l_{\text{disp}}^2 = \frac{1}{12}\lambda_D^2\kappa^2,$$
$$\Lambda = -(\kappa^3 + 3\kappa^2 + 6\kappa + 6)/(\kappa^2 + 2\kappa + 2).$$

In the opposite case of $\kappa \ll 1$,

$$C_{DL}^2 = \frac{Q^2}{m\lambda_D}[3 + 2\ln(\kappa^{-1})]/\kappa,$$
$$l_{\rm disp}^2 = \lambda_D^2/[3 + 2\ln(\kappa^{-1})],$$
$$\Lambda = -[11 + 6\ln(\kappa^{-1})]/[3 + 2\ln(\kappa^{-1})].$$

In the weakly inhomogeneous case, when the lattice parameters change on a scale much larger than the size of the soliton, we can use a locally homogeneous equation with the kinetic coefficients having parametric dependencies on the coordinate:

$$\ddot{u} + \nu_d\dot{u} = C_{DL}^2(u'' + \Lambda u'u'' + l_{\rm disp}^2 u''''), \qquad (3)$$

where dots and primes denote partial time and space derivatives, respectively. We do not study the influence of the boundaries, i.e., consider the infinite medium.

The friction is weak and, for a compressional disturbance propagating with a speed $C = 20$–40 mm/s, the damping length is $C/\nu_d \simeq 9$–15 mm which is much larger than the width of the disturbance. Therefore we can omit the friction term in the first approximation. Then, Eq. (3) has soliton solutions for the particle velocity: $v = \dot{u} = CA\cosh^{-2}(\xi/L)$, where $\xi = x - Ct$ is a self-similar variable, C is the soliton velocity, A is the dimensionless soliton amplitude, and L is the soliton width. The particle displacement can be expressed as $u = AL[1 - \tanh(\xi/L)]$ and the compression factor as

$$n/n_0 = (1 + u')^{-1}. \qquad (4)$$

The relations between the soliton parameters A, L, and M are well known in this case:

$$M^2 - 1 = 4l_{\rm disp}^2/L^2 = -\Lambda A/3. \qquad (5)$$

As the soliton amplitude increases, the speed also increases, and the width decreases since $AL^2 = \text{const}$. The continuum limit approximation is valid when $L \gg a$. Applying Eq. (5) we obtain the condition for Mach number $M^2 - 1 \ll (4/\kappa^2)(l_{\rm disp}^2/\lambda_D^2)$. For our experiment $\kappa \approx 1$ and this condition is equivalent to $M - 1 \ll 1$.

We used the compression factor n/n_0 from Eq. (4) to fit the experimental data (Fig. 3). It turned out that the best fits were obtained using a sum of two soliton solutions where the first soliton has a higher amplitude and propagated faster than the second one. It corresponds to the dark feature marked with a dashed curve in Fig. 2. The second soliton is barely noticeable in Fig. 2 as a slightly darker feature above the main soliton. It separates from the first soliton at about 15 mm and lags 0.3 s behind at 30 mm. The amplitude of both solitons decreases in time due to damping.

Note that the compression factor in Fig. 3 decreases to the left of the soliton (closer to the wire). Since, in our case, the lattice has a finite size and is confined in a parabolic potential, it is shifted from its equilibrium position as the soliton passes through. After the soliton has passed, the particles return to their equilibrium positions reducing the compression factor behind, i.e., to the left of the soliton.

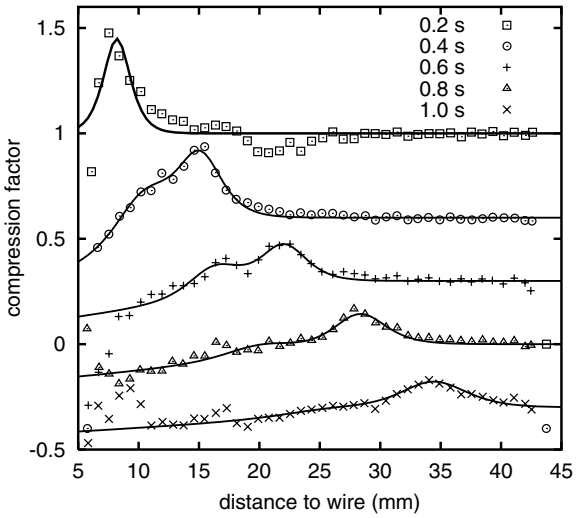

FIG. 3. Compression factor n/n_0 versus distance to the wire at different times. The solid lines show the theoretical fits to the experimental data. Two solitons are present. The fits and experimental points at later times are offset down (by 0.4, 0.7, 1.0, 1.3, respectively).

In making the fits, we took into account this backflow of the lattice. We assumed that the horizontal confining potential is $U_{\rm ext} = m\Omega_o^2 x^2/2$, where Ω_o is the horizontal oscillation frequency. In our case $\Omega_o/2\pi = 1.2\ {\rm s}^{-1}$, $L \approx 3$ mm, and $C \approx 30$ mm/s. The soliton characteristic time scale $L/C \ll 1/\Omega_o$. Thus we can neglect the influence of the backflow on the soliton shape and separate the soliton solution from the baseline.

The restoring force is $F_{\rm ext} = -m\Omega_o^2\delta u$, where δu is the displacement due to the soliton. Solving the equation of motion leaving only the acceleration, the wave, and the external force terms, we obtained the velocity gradient of the restoring motion:

$$v'_{rm} = \Omega_o^2 C\delta u/(C^2 - C_{DL}^2), \qquad v_{rm} = \dot{u}. \qquad (6)$$

Applying the continuity equation to Eq. (6) yields the reduction of the compression factor. This solution is valid near the soliton at a distance smaller than the damping length and is good as a first approximation.

The relations between the soliton amplitude and width including inhomogeneity and damping were calculated by applying the energy conservation to Eq. (2):

$$\frac{dW}{dt} = -2\nu_d K, \qquad K = \frac{m}{2}\int_{-\infty}^{+\infty}\frac{\dot{u}^2}{\kappa}\frac{dx}{\lambda},$$

$$P = \frac{m}{2}\int_{-\infty}^{+\infty}\frac{C_{DL}^2}{\kappa}[u'^2 + \Lambda u'^3/3 - l_{\rm disp}^2 u''^2]\frac{dx}{\lambda_D}, \qquad (7)$$

where K, P, and $W = K + P$ are kinetic, potential, and total energy, respectively. Substituting the soliton solution for u into Eq. (7) we obtain that $W = (2\alpha/5)(4M^2 + 1)(A^2L)$ and $K = \alpha M^2(A^2L)$, where $\alpha = (2/3)mC_{DL}^2/(\kappa\lambda_D)$. In case $M - 1 \ll 1$ (when

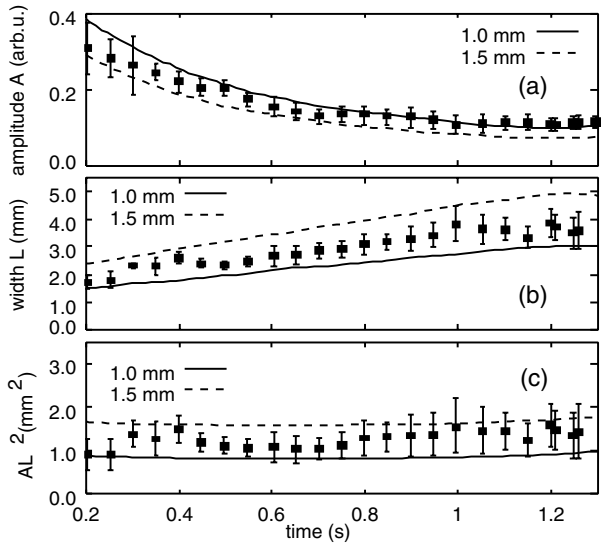

FIG. 4. Amplitude A (a), width L (b), and soliton parameter AL^2 (c) as a function of time for the larger soliton. The soliton parameter is approximately constant. The dots are the experimental data. The lines correspond to the theory at different screening lengths.

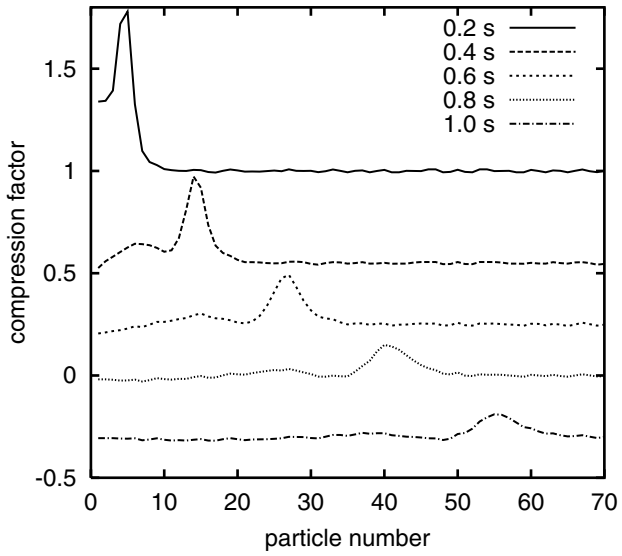

FIG. 5. Compression factor versus particle number for a simulated linear chain model. It describes the formation of two (or more) solitons by a single excitation pulse and qualitatively agrees with the experiment. The curves at later times are offset down (by 0.45, 0.75, 1.0, and 1.3, respectively).

the continuum limit is applicable) $W \approx 2K$ and the total energy decays exponentially, $W \propto \exp(-\nu_d t)$. The soliton amplitude and width are related to the total energy by $W \approx 2\alpha(A^2 L)$, and they also scale exponentially as

$$A \propto \exp(-2\nu_d t/3), \qquad L \propto \exp(\nu_d t/3)\,.$$

The soliton parameters A, L, and AL^2 determined from the experiment for the first (larger) soliton are plotted in Fig. 4. Note that the parameter $AL^2 \approx$ const in the weakly damped inhomogeneous case. Lines in Fig. 4 show the full solutions of Eqs. (7) for two different values of λ_D. Our case corresponds to the screening length of $\approx$1.2 mm.

The analytical model presented here does not describe the formation of multiple solitons by a single pulse. However, two solitons were observed in a molecular dynamics simulation of a linear inhomogeneous chain which we performed. The confining potential for 100 particles was chosen to get a distribution of the number density similar to the experiment. Varying the excitation pulse we achieved a qualitative agreement with the experiment (Figs. 5 and 3). The simulation parameters are $Q = 1.6 \times 10^4 e$, $\Omega_o = 1.2$ s, $\nu_d = 2.4\ \mathrm{s}^{-1}$, $\lambda_D = 1$ mm, and excitation time 0.1 s. The simulation produced different numbers of solitons depending on the excitation; e.g., we were able to obtain more than two solitons by increasing the excitation length. This was also observed in the experiment when the amplitude of the excitation pulse was increased.

Here we have presented an experimental study of dissipative longitudinal solitons in a monolayer hexagonal dust lattice. A simple linear chain theory taking into account damping and inhomogeneity was suggested to describe the experiment. A linear chain simulation reproduced the formation of multiple solitons by a single excitation pulse. The theory and the simulation agree qualitatively with the experiment. A full two-dimensional soliton model is a subject of our future work.

*Email address: dima@mpe.mpg.de

[1] J. Robinson and J. Russel, in *Report of the Committee on Waves, Report of the 7th Meeting of British Association for the Advancement of Science* (John Murray, London, Liverpool, 1838), p. 417.
[2] D. Korteweg and G. de Vries, Philos. Mag. **39**, 422 (1895).
[3] N. Rao, P. Shukla, and M. Yu, Planet. Space Sci. **38**, 543 (1990).
[4] A. V. Ivlev and G. Morfill, Phys. Rev. E **63**, 026412 (2001); **63**, 026412 (2001).
[5] F. Melandsø, Phys. Plasmas **3**, 3890 (1996).
[6] H.-Y. Hao and H. Maris, Phys. Rev. B **64**, 064302 (2001).
[7] H. Thomas, G. Morfill, V. Demmel, J. Goree, B. Feuerbacher, and D. Möhlmann, Phys. Rev. Lett. **73**, 652 (1994).
[8] J. Maddox, Nature (London) **370**, 411 (1994).
[9] D. Samsonov, A. Ivlev, G. Morfill, and J. Goree, Phys. Rev. E **63**, 025401(R) (2001).
[10] A. Homann, A. Melzer, R. Madani, and A. Piel, Phys. Lett. A **173**, 242 (1998).